THE ASTROPHYSICAL JOURNAL, 336:128–139, 1989 January 1

QUANTIZATION OF REDSHIFT DIFFERENCES IN ISOLATED GALAXY PAIRS

W. G. TIFFT AND W. J. COCKE
Steward Observatory, University of Arizona
Received 1987 December 28; accepted 1988 June 18

ABSTRACT

Improved 21 cm data on isolated galaxy pairs eliminates questions of inhomogeneity in the data and reduces observational error to below 5 km s^{-1}. Quantization is sharpened, and the "zero" peak is shown to be displaced from zero to a location near 24 km s^{-1}. An exclusion principle is suggested whereby identical redshifts are forbidden in limited volumes. New southern hemisphere optical data from L. Schweizer are also found to be consistent with quantization and the avoidance of zero differentials. The radio and Schweizer data are combined with the best optical data on close Karachentsev pairs to provide a cumulative sample of 84 of the best differentials now available. New 21 cm observations are used to test for the presence of small differentials in very wide pairs. The deficiency near zero is found to continue to very wide spacings. A loss of wide pairs by selection bias cannot produce the observed zero deficiency. A new test using pairs selected from the Fisher-Tully catalog is used to demonstrate quantization properties of third components associated with possible pairs.

Subject headings: galaxies: redshifts — radio sources: 21 cm radiation

I. INTRODUCTION

Although quantization has now been demonstrated for a variety of galaxy samples (Tifft 1980, 1982*a*, *c*, 1987; Cocke and Tifft 1983; Tifft and Cocke 1984; Sharp 1984; Arp and Sulentic 1985; Arp 1986; Napier 1988), the basic test using isolated galaxy pairs remains of central importance. For such elementary pairs the form of the quantization appears to approximate a simple periodicity of 72.45 km s^{-1}. The test provides a strong contrast with ordinary dynamical predictions of a continuous distribution of differentials peaking at zero. Since the discussions of pairs in 1980–1982 several new developments have occurred. New 21 cm data have been obtained in order to improve internal consistency and accuracy of the radio sample, and to test specifically for effects relating to wide pairs. A new optical sample of southern pairs has also been published by Schweizer (1987). In § II we discuss 21 cm data. Section III concerns new optical data. Section IV incorporates older optical data and presents a cumulative distribution of 84 pairs to illustrate the variety of data which support a quantum model. Section V concerns radio studies of wide pairs and diffuse groups in a search for small differentials which could be overlooked by selection biases. Section VI develops a new quantization test using triplets and small systems of galaxies. An appendix contains an error analysis comparing the data of Karchentsev (1980) and Tifft (1982*b*) on differential redshifts.

As the investigation of quantization effects develops, it is increasingly important to draw basic distinctions between quantum models and ordinary dynamical models of the redshift. This paper introduces and develops new concepts relevant to a quantum model which must be judged from the data, not from dynamical expectations. Effects of sample selection, data quality, and physical or velocity separation are quite different in the two approaches. The basic groundwork for quantization modeling was developed, and a set of predictions made, in the mid-1970s (Tifft 1976, 1977*a*, *b*) before any of the present data existed.

II. PAIRS AT 21 CENTIMETERS

The first independent test of the original quantization predictions (Tifft 1976, 1977*a*, *b*) utilized a sample of pairs defined by Peterson (1979). Peterson obtained numerous 21 cm redshifts and supplemented them with optical data from outside sources. There are several problems with the Peterson sample. The quality of the optical data included was overestimated, while uncertainty in the radio data itself was not actually known. Several pairs are definitely not isolated, and a sizable contamination from accidental pairing within diffuse groups is almost certainly present, since a number of the pairs have very large projected spacings. Some of these factors were discussed in the original quantization paper (Tifft 1980); however, questions continue to be raised about the significance of the original study. In Table 1 we list the 31 Peterson pairs for which Peterson provided 21 cm data for both components and for which ΔV is less than 500 km s^{-1}. The pairs are identified by UGC number and are ordered in ΔV. Deviations from standard values are given in parentheses following the ΔV values. Specific problems are identified for a number of the pairs. Pairs with contamination by obvious companions, with projected spacings wider than about 300 kpc (for $H = 75$ km s^{-1} Mpc^{-1}), and with $\Delta V > 350$ km s^{-1} are identified. Contamination of pairs by accidental associations within diffuse physical groups is now recognized as a basic problem for identification of true physical pairs (Sadler and Sharp 1984; Picchio and Tanzella-Nitti 1985). Contamination increases as separation in both space and velocity increases. The Peterson pairs with $\Delta V < 350$ km s^{-1} and projected spacings below 300 kpc, and without obvious secondary companions, show a 16.5:4.5 fit to quantization predictions. The specific binning used is based upon previous predictions or observations (Tifft 1976; Tifft and Cocke 1984) and is discussed further below. The bins and boundary values are indicated in the table. The subset most likely contaminated by interlopers divides equally. It is clear that the Peterson radio data show the predicted

TABLE 1

PURE RADIO PAIRS FROM PETERSON

UGC	ΔV (km s^{-1}) In	ΔV (km s^{-1}) Out	BOUND (km s^{-1})	BIN	MAJOR PROBLEMS
12883/12889		1		0	Spacing > 300 kpc
1070/1078		10			
			12		
9615/9628	13(−11)			1/3	
8507/8516	14(−10)				
89/94	16(−8)				
4066/4151	16(−8)				
8792/8809	17(−7)				Not isolated!
5520/5576	19(−5)				Spacing > 300 kpc
11137/11144	19(−5)				Spacing > 300 kpc
7111/7116	20(−4)				
8396/8403	26(+2)				
			36		
				2/3	
5251/5280	60(−12)		60		
7721/7732	68(−4)			1	
8699/8700	68(−4)				
9908/9915	69(−3)				
5279/5292	73(+1)				
9797/9805	83(+11)				
			91		
10848/10897		97(+25)		1.5	
1541/1550		117(−27)			
7407/7414		123(−21)			
			127		
12607/12610	137(−7)			2	
725/728	140(−4)				
9493/9499	158(+14)				
			163		
1759/1768		173(+29)		2.5	Not isolated!
10628/10656		196(−20)			Spacing > 300 kpc
			199		
4593/4603	201(−15)			3	
3930/3937	210(−6)				Spacing > 300 kpc
7706/7747	232(+16)				Spacing plus companion
			235		
				3.5	
			272		
9347/9361	299(+10)			4	
			308		
				4.5	
			344		
				5	
			380		
4752/4794		391(+30)		5.5	Large spacing and V
7685/7694		401(−32)			Large velocity
			417		

quantization for those systems which are most likely to be physical pairs.

Following the original Peterson pair analysis, a revised sample was defined (Tifft 1982*a*) which eliminated the obvious contamination and very wide pairs discussed above. The sample was also extended to include additional isolated pairs with 21 cm data. The primary drawback of the sample, which fully confirmed the Peterson sample results, was that radio data, and occasionally high-quality optical data, from a variety of sources was combined. Questions concerning the homogeneity of the final data therefore remained. This sample, subsequently referred to as the revised radio sample, was therefore included in a study, begun in 1984, to examine 21 cm redshift precision. Results of observations done at the 91 m NRAO[1] telescope at Green Bank have now been published (Tifft and Cocke 1988). Table 2 and Figure 1 summarize the results for those objects which have separations greater than 12′, sufficient for adequate isolation by the 10.′8 beam of the 91 m telescope. UGC identifications, heliocentric redshifts, and differentials, after correction for solar motion (Tifft and Cocke 1984), are listed, as are signal-to-noise ratios. One object, with a very low signal-to-noise ratio, is within the 72 km s^{-1} peak but is omitted from Figure 1. One object with spacing less than

[1] The National Radio Astronomy Observatory is operated by Associated Universities, Inc., under contract with the National Science Foundation.

TABLE 2

NEW 21 CENTIMETER DATA FOR ISOLATED PAIRS

UGC	V_h (km s^{-1})	ΔV (km s^{-1})	S/N	
1070/1078	2806.6/2782.2	24.0	16	8
3809/3834	2204.1/2038.4	165.4	55	30
4066/4151	2296.7/2286.5	11.1	25	11
5251/5280	1478.8/1545.1	66.5	62	18
5279/5292	1486.4/1555.2:	:	10	2
6116/6123	1132.1/ 979.8	151.1	12	19
7111/7116	1309.8/1327.4	18.4	27	39
7154/7166	1011.2/ 999.5	13.3	30	46
7721/7732	1735.8/1808.2	70.6	26	26
7853/7861	544.2/ 609.2	65.4:	65	19
8396/8403	948.5/ 970.6	22.9	13	40
8507/8516	993.6/1019.4	28.1	6	7
8699/8700	2521.9/2572.5	51.0	7	7
9493/9499	1569.6/1723.0	153.8	20	9
9615/9628	1801.4/1787.3	14.3	12	9
9797/9805	3391.7/3312.8	77.8	70	11
9908/9915	1898.5/1826.7	70.2	7	29
10848/10897.....	1259.7/1318.6	59.7	6	42
12732/12754.....	747.4/ 749.4	0.9	182	52

the beam size is flagged as less certain. For the remaining objects, multiple observations and external comparisons demonstrate excellent consistency. Measures are consistently reliable to better than 5 km s^{-1} at the signal levels involved. A detailed discussion of 21 cm uncertainties will be published elsewhere.

The first section of Figure 1 shows the redshift differential distribution of the complete revised radio sample as published in 1982. The second section shows the portion which could be reobserved at the 91 m telescope. The third line shows the new data. Two conclusions follow from this study. First, the scatter of points is reduced, and quantized values sharpen. Scatter is now dominated by real differences and by how well a 21 cm measurement represents the actual center-of-mass redshift of a galaxy. Second, the "zero" peak is not at zero. Using conservative 5 km s^{-1} uncertainties, all but one of the points in the lowest peak deviate from zero by more than 2 σ. We conclude that zero is in fact avoided. If our quantum model is correct, it appears that an exclusion principle may be operating, such that identical redshifts may not coexist in the spatial volumes involved. Previous studies in groups (Cocke and Tifft 1983) had suggested such a deviation, but the data quality was not sufficient to allow specific conclusions. Further definition of the precise location and form of peaks will require higher resolution data, since the remaining pairs, especially at the 145 km s^{-1} peak, have angular spacings too close for the 91 m telescope beam.

We make no attempt here to discuss the formal significance of quantization in the new radio data, since the data are incomplete and have been used to recognize the zero deviation. Pending more detailed studies of the exact location of the first peak, we adopt 72.45/3 = 24.15 km s^{-1} as its location because of the significance of this submultiple in global quantization work (Tifft and Cocke 1984). The strong 24 km s^{-1} global quantization could be explained if 24 km s^{-1} offsets occur within the 72 km s^{-1} periodicity. It was shown (Fig. 8 of Tifft and Cocke 1984) that dwarf galaxies can be represented by a 72 km s^{-1} periodicity with lower population wings 24 km s^{-1} on either side. A 24 km s^{-1} zero offset could generate such a pattern and explain why this period dominates globally. The zero deviation effect by itself has particularly important consequences as a fundamental test of the applicability of conventional dynamics to binary galaxies. Newtonian dynamics requires a peak at zero. Selection effects, discussed further in § V, could modify the zero peak predicted by dynamics, but not remove it completely. Evidence for an unexpected dip at zero is

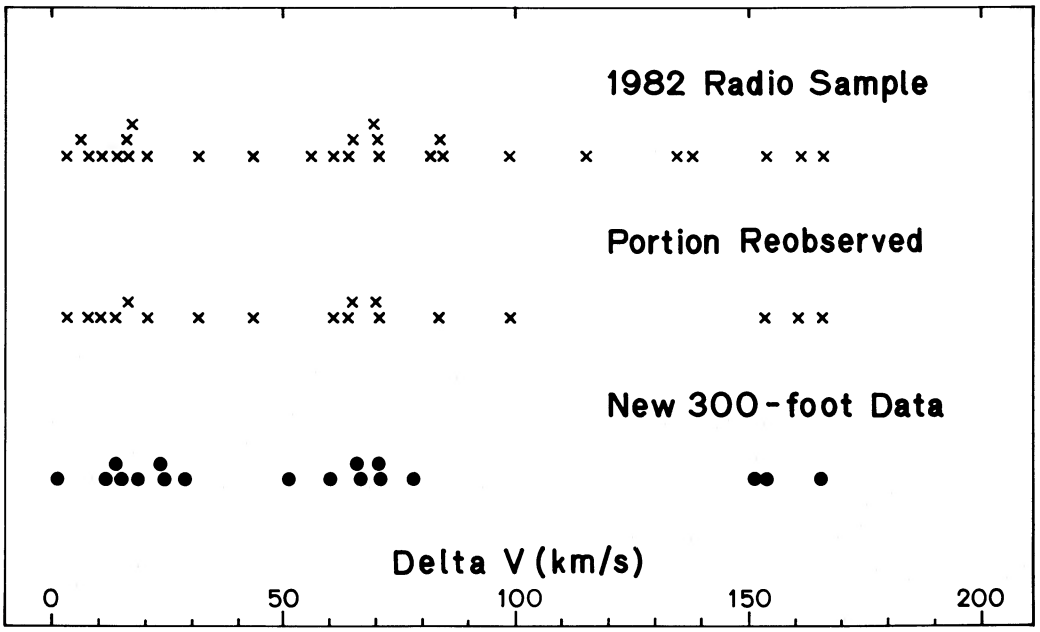

FIG. 1.—(*Top*) Differential redshift distribution of the revised radio sample as published in 1982. (*Middle*) Pairs in the sample which are adequately resolved with the 91 m NRAO telescope. (*Bottom*) New accurate 21 cm redshift differentials for the pairs on the second line.

not limited to the work reported here. White *et al.* (1983) noted an unexpected deficiency in the Turner (1976) sample.

III. NEW OPTICAL DATA

A new set of southern hemisphere binary galaxies has been studied by Schweizer (1987). Typical redshift uncertainty near 9 km s^{-1} is indicated, and differentials should therefore have uncertainties of 13 km s^{-1}. The sample provides a critical independent test for quantization in pairs. One difficulty with the sample is that it includes a sizable number of rather wide pairs. Figure 2 shows the distribution of the Schweizer objects superposed on the high-weight Karachentsev systems from Tifft (1982*b*) for which quantization has been demonstrated (Tifft 1982*c*; Sharp 1984). The diagram shows ΔV versus the product of the mean system redshift and the angular separation VS, which is proportional to the projected physical spacing. The Karachentsev sample contains only one object with $VS > 300$ km s^{-1} deg, while the Schweizer sample contains 11. In § VI of this paper we will examine the quantization behavior of such pairs. Initially we will restrict our comparison to the region below 300 km s^{-1} deg, where the samples correspond well, and where the properties of quantization are established. Since pair quantization has also not been demonstrated beyond the fourth level, we limit our initial comparison to the velocity range below 350 km s^{-1}. We refer to this region, where the Schweizer and Karachentsev samples must be consistent, as the critical region.

Table 3 lists the Schweizer systems, in ΔV order, for the critical region. Predicted bins are indicated centered at multiples of 72.45 km s^{-1} except for the "zero" bin now centered at 24.15 km s^{-1} as shown by the radio studies. Each differential is followed by its deviation, in kilometers per second, from the nearest predicted value. To retain equal in and out bin areas for testing, the 72 km s^{-1} bin cannot be symmetrical about the predicted value. The Schweizer data conform to the predicted bins in a 20.5:6.5 = 3.1 ratio. This ratio has a formal probability of occurrence of only 0.007, compared with the conventionally expected ratio of 1.0. For a discussion of statistical methods utilized in In:Out (I:O) comparisons see Tifft (1982*c*), Tifft and Cocke (1984), and Sharp (1984). Figure 3 shows the ΔV distribution of the critical sample, including a detailed picture of the test region with error bars attached to the points. The points are distributed statistically just as required with respect to the predicted quantum levels. Intermediate values, or a value of zero, are statistically incompatible with the error distributions. The I:O ratio is near the maximum value possible for the uncertainties associated with the Schweizer data (Tifft 1982*c*). We have complete consistency in the region defined by the sample of close Karachentsev pairs.

When we examine the data outside the close-pair domain, there is a change. Table 4 contains the (I:O) ratios for the wider-spaced, larger ΔV data. The rejected radio pairs are included for comparison. The wider Schweizer pairs have typical projected spacings near 100 kpc for $H = 75$ km s^{-1} Mpc^{-1}. This is less than the cutoff limit for the radio pairs, but well outside the region occupied by the close Karachentsev pairs. Further discussion of quantization behavior at wide spacings is deferred to §§ V and VI of this paper.

IV. OTHER DATA AND THE CUMULATIVE DISTRIBUTION

The only other pair sample large enough and of sufficient precision to investigate quantization is the sample of isolated Karachentsev pairs used in the previous section to define the test region for the Schweizer pairs. An extensive internal error analysis was carried out at the time of publication (Tifft 1982*b*).

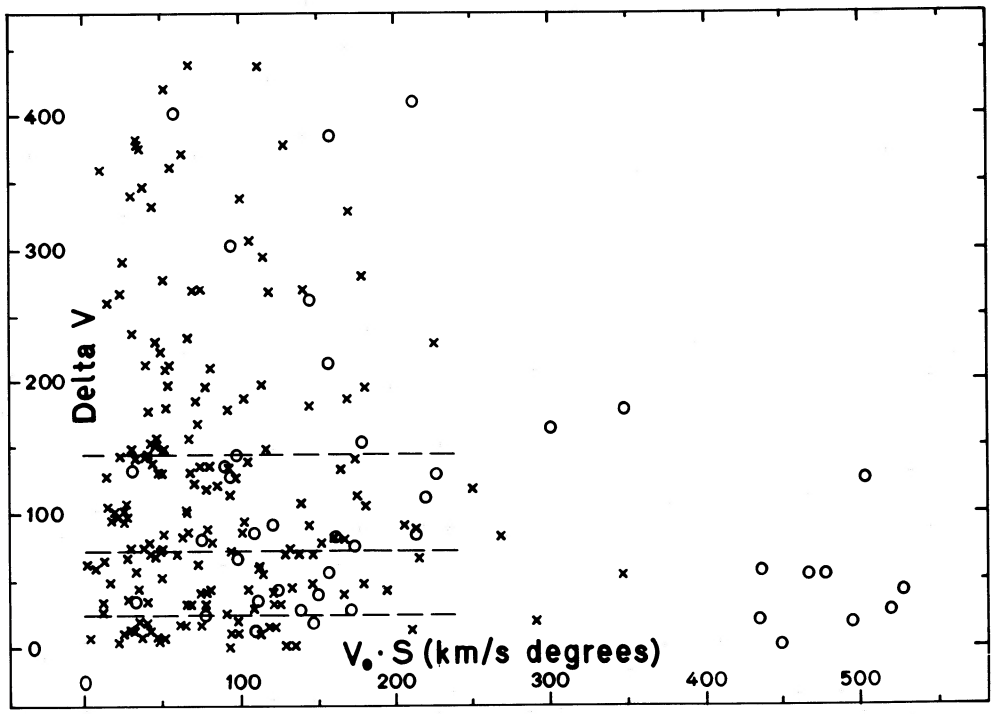

FIG. 2.—Distribution of the Schweizer pairs (*open circles*) compared with the high-weight Karachentsev pairs with $\Delta V < 450$ km s^{-1} (*crosses*). The ordinate is the redshift differential. The abscissa, the product of the mean galactocentric redshift and the angular separation of the pair, is proportional to projected physical spacing.

TABLE 3

PAIRS FROM SCHWEIZER

PAIR	ΔV (km s^{-1}) In	ΔV (km s^{-1}) Out	BOUND (km s^{-1})	BIN
			0	
				0
33	12(−12)		12	
13	18(−6)			1/3
47	24(0)			
20	28(+4)			
34	28(+4)			
7	35(+11)			
43	35(+11)			
			36	
30		40(+16)		2/3
3		43(−29)		
8		56(−16)		
			60	
25	67(−5)			1
29	75(+3)			
12	81(+9)			
24	83(+11)			
26	85(+13)			
14	86(+14)			
			91	
15		93(+21)		1.5
32		112(−33)		
			127	
16	128(−17)			2
5	130(−15)			
2	134(−11)			
46	136(−9)			
31	145(0)			
9	154(+9)			
			163	
				2.5
			199	
35	214(−3)			3
			235	
17		262(−28)		3.5
			272	
44	303(+13)			4
			308	
				4.5
			344	
				5
			380	

About 200 pairs are classified as "high-weight pairs," and it is only among these that sufficient precision is obtained to study quantization. Within the high-weight pairs there are variations in uncertainty depending upon the type and clarity of spectral features present and upon the pair separations. The ability to detect a periodicity depends directly on the blurring from data uncertainty. Tifft (1982*c*) demonstrated that the level at which quantization was detectable in various subsamples was consistent with the estimated uncertainties. The internal estimates and the quantization visibility indicate that the better differentials achieve uncertainties near 20 km s^{-1}. No equivalent set of data exists for a direct external error check. Karachentsev (1980) gives redshifts for some pairs in common, mostly emission-line objects. An Appendix to this paper presents a comparison with the Karachentsev data. The comparison is consistent with the uncertainties determined by Tifft.

As discussed in the Appendix and by Tifft (1982*c*), we can minimize uncertainty and maximize the visibility of the quantization if we use pure common-line emission and common-line absorption pairs with separations less than 40″. Data for pairs with mixed absorption and emission or at wider spacing are clearly of lower quality. In addition, at very small spacings some confusion exists between true pairs and parts of a single object. To eliminate this confusion, we will also adopt a lower projected physical spacing of about 7 kpc (for $H = 75$ km s^{-1} Mpc^{-1}). Forty-one pairs have $\Delta V < 300$ km s^{-1} and satisfy all the optimization criteria. In Figure 4 we combine this subsample with the Schweizer and new radio data, as discussed above, to give a total sample of 84 of the most reliable pairs with ΔV less than 250 km s^{-1}. The purpose of this exercise is simply to give an overall impression of the present status of pair quantization work. No statistical analysis of such a mixed sample is possible; however, analysis of each sample individually has been shown to yield significant results. Evidence for quantization extends over a wide range of spacings and involves data obtained by very different techniques, optical and radio. Four maxima and four minima are presently detectable in the distribution of redshift differentials for isolated pairs.

TABLE 4

IN:OUT DISTRIBUTION OF REJECTED PAIRS

Sample	In	Out	Reason for Rejection
Radio	4	2	Large *VS*
	0	1	$\Delta V > 350$
	0	1	Both reasons
Schweizer	4	7	Large *VS*
	0	3[a]	$\Delta V > 350$

[a] The Schweizer complete sample also includes seven with $\Delta V > 500$ km s^{-1}, of which five have $\Delta V > 2000$ km s^{-1}.

V. SELECTION IN WIDE PAIRS

The theoretical form of the ΔV distribution for a complete and uncontaminated set of galaxy pairs is easily shown (Tifft 1977*a*) to be a monotonic distribution peaking at zero in a conventional dynamical framework. The form arises from projection effects and is independent of orbital characteristics for an isotropic distribution. In a real sample, selection may modify the distribution, although no known effects can produce multiple peaks or a distinct minimum at zero, since most values can occur at any separation. Two radial regions are recognized where objects will be lost preferentially: very small separations where confusion from superposition enters, and very wide separations where companions mix with unrelated galaxies. The first effect involves relatively few pairs and will not be discussed here. The effect has been discussed by Schweizer (1987) and found to be small. Because of field confusion, no comprehensive study at large spacings has been done. Within the region which has been studied no dependence of the ΔV distribution on separation is apparent, and most studies have found that the distribution is nearly independent of spacing. A test dividing the Karachentsev pairs by separation to introduce a deliberate strong bias (Tifft 1982*c*) shows no effect.

Since the frequency distributions of physical spacings and orbital eccentricity are not known, one cannot predict in detail what effect selection will have on observed distributions. It is possible, however, to observe a set of wide pairs and find the ΔV distribution of objects available to modify the physical pair

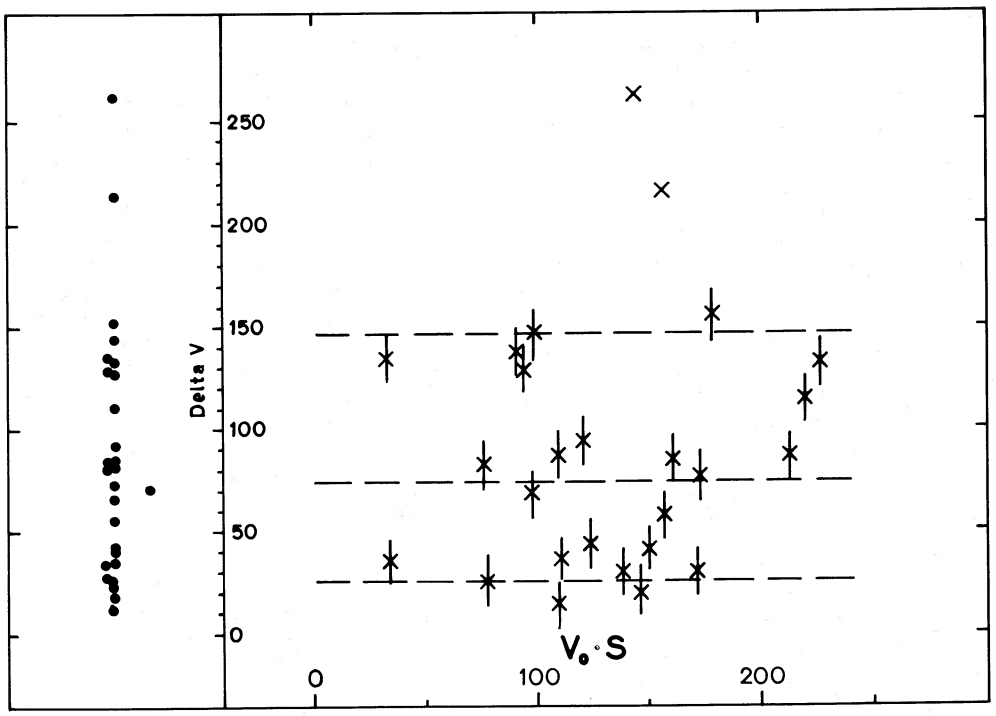

FIG. 3.—Distribution of the Schweizer pairs in the test region below $VS = 300$ km s^{-1} deg. The ΔV distribution on the left is displayed as a function of projected physical spacing on the right. One sigma (13 km s^{-1}) error bars are attached to the points to illustrate the statistical compatibility of the data with the principal quantization levels, shown as dashed lines.

distribution. In particular, if an excess of objects with very small ΔV were present to compensate for the large deficiency seen at zero, it should be easily observable.

The distribution of galaxies is known to be distinctly lumpy, with most galaxies associated in loose groups, leaving few unbound field objects. When one chooses relatively close pairs at small ΔV, one is selecting almost entirely either physical pairs or accidental pairs within physical groups. Since the groups are apparently bound, the velocity distribution should be roughly Gaussian, as is in fact observed. Within a conventional dynamical framework random pairs selected from such a distribution should have a ΔV distribution which peaks at zero. It therefore makes little difference whether wide pairs are physical pairs or are accidental within groups; a peaking of ΔV at zero is still expected. For the randomized-motion pattern in groups there should also be no important selection effects as a function of separation.

The situation is different for a quantization model. The presence of a zero-exclusion condition will presumably restrict differentials within groups as well as between pairs, depending upon the volume over which the exclusion applies. A zero deficiency may therefore be expected, inside restricted volumes, for differentials within groups. Even though an overall velocity distribution appears roughly Gaussian, pairing within a quantum model is restricted and the differential pattern assumes a special form. The existence of a specific velocity envelope does not demonstrate that conventional dynamics is sufficient to explain the details of the distribution. The presence

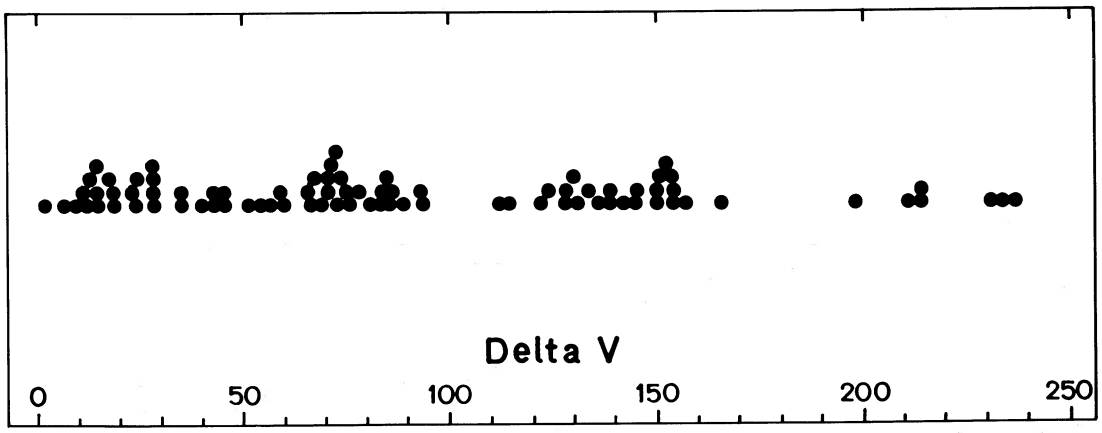

FIG. 4.—Cumulative differential redshift distribution of 84 points from the three best data sets, the revised radio sample (18), the Schweizer sample (25), and the high-weight Karachentsev pairs (41).

of a consistent differential structure raises serious questions concerning large-scale gravitational dynamics.

To test the form of the ΔV distribution in wide pairs, the Fisher-Tully (1981) catalog was searched for candidate pairs. For each galaxy, companions with small projected physical spacing were identified. The list includes many combinations in the spacing range from 200 kpc to 1 Mpc, well outside the region examined for physical pairs. From this set of pairings, combinations with $\Delta V < 50$ km s^{-1} were identified. Objects from this list were included, whenever possible, in the new study to obtain accurate redshifts. Figure 5 shows the differential distribution for all such combinations, with a VS product between 860 and 3600 km s^{-1} deg, which could be formed from the full list of galaxies appearing in the final catalog of new redshifts (Tifft and Cocke 1988). The distribution does not peak at zero despite the fact that most of the differentials must come from within physical groups and we have picked the smallest differentials available. The interval 14–28 km s^{-1} shows a factor of 1.5 enhancement compared with 0–14 km s^{-1}. The location of the new Tifft-Cocke radio pairs, and the Schweizer pairs as discussed above, is shown with crosses for the 24 km s^{-1} quantum level. The enhanced ΔV interval for general wide pairs differs little from the lowest level in isolated pairs. The common argument that a zero deficiency can be produced by a selective omission of wide pairs is obviously not supported.

VI. EFFECTS OF THIRD COMPONENTS

The previous discussion suggests that a redshift exclusion concept could extend to spatial volumes much larger than the small volumes we have considered with isolated pairs. This permits some predictions concerning the pattern of differentials to be found within groups of a few objects. If we add a third galaxy to a pair, it presumably must be offset from both. The pattern of redshift differences within primary pairs and between members of primary pairs and third objects should be different. For small differentials in particular, we might expect a multiplicity of the 24 km s^{-1} zero offsets to appear. To test this, the Fisher-Tully catalog (1981) was searched for all pairs with $\Delta V < 108$ km s^{-1} (1.5 × 72) and with a VS product less than 500 km s^{-1} deg. There are 44 such pairs listed in Table 5, where they are identified by UGC, NGC, or "anon" right ascension code. Angular separations are indicated, and objects with new data have the Tifft-Cocke (1988) serial numbers listed. ΔV is formed from the Tifft-Cocke (T) or Fisher-Tully (F) redshifts, after solar-motion corrections (Tifft and Cocke 1984). The ΔV limit restricts the test to the two critical well-populated lowest levels, while the VS limit restricts the test to the spatial volume which contains demonstrated quantization. The pairings divide into two categories, which we designate reciprocal or nonreciprocal. Reciprocal pairs are pairs where each galaxy finds the other to be its nearest neighbor. For nonreciprocal pairs one or both galaxies find that other galaxies are closer. Reciprocal pairs will include real primary physical pairs, but since the catalog is not complete, some must be unrecognized nonreciprocal pairs. Many differentials from such pairs may therefore fit the standard levels, but the sample will be contaminated. A closely spaced nonreciprocal pair, on the other hand, is unlikely to be an isolated physical pair, so the differential will be a good candidate for one involving a third object. Differentials in such combinations should be preferentially offset from the standard quantum levels. Figure 6 shows the distribution of the reciprocal and nonreciprocal differentials for the 44-pair Fisher-Tully sample. The total sample has a distinct zero deficiency but no obvious higher periodicities. Periodicities appear as soon as we distinguish by reciprocity. The 29 reciprocal pairs, despite contamination, yield I/O = 2.6, which by itself confirms quantization at the 98% confidence level. The 15 nonreciprocal pairs have the opposite distribution. O/I = 2.8, thus a clear preference for the expected offset locations. Five pairs in the list overlap other quantization studies as indicated in the last column of Table 5 (Groups: Cocke and Tifft 1983; Pairs: Tifft 1982*a*).

The test confirms the exclusion concept and demonstrates the importance of distinguishing isolated pairs for critical testing in the primary intervals. It illustrates some of the complications to be expected in studies of groups and in wide pairs, where subtle third-party contamination becomes important. On the other hand, it opens the way for more formally defined tests using third components and small systems of galaxies. A more detailed discussion of groups is currently beyond the scope of this paper. Some recent work, including work with clusters, is discussed elsewhere (Tifft 1987). Groups and clusters are basic to quantization studies (see, for example, Schneider *et*

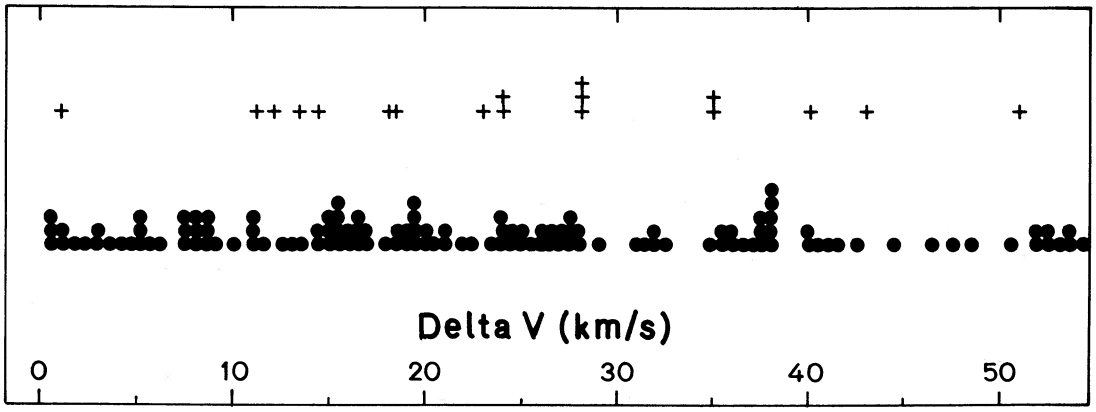

FIG. 5.—ΔV distribution of all pairs (*filled circles*) with VS products between 860 and 3600 km s^{-1} deg and $\Delta V < 55$ km s^{-1} within the new 21 cm data. Plus signs indicate the revised radio and Schweizer pairs associated with the 24 km s^{-1} quantization level. The observations deliberately emphasized small differentials, and the distribution does not rise toward zero.

TABLE 5

CATALOG PAIRS FROM FISHER-TULLY

UGC	Tifft-Cocke	S	VS (km s^{-1} deg)	Category[a]	ΔV (km s^{-1})	Reference[b]	Overlap
1195/1201	441/443	0°37	339.7	r	76.9	TT	
1807/1831	30/454	0.48	361.0	r	99.5	TT	
A0909/N2781	112	0.24	440.8	r	19.6	TF	
A0941/A0942	...	0.39	400.0	r	47.4	FF	
6079/6126	150/154	0.70	471.8	r	23.7	TT	Groups
N3511/N3513	...	0.18	168.9	r	90.5	FF	
6328/6346	160/162	0.33	229.1	r	80.1	TT	Groups
6328/6350	160/163	0.60	450.9	n	43.7	TT	Groups
6815/6840	183	0.33	357.4	r	42.7	FT	
6840/6870	...	0.34	383.8	n	36.0	FF	
6923/6937	184	0.23	260.8	r	13.0	TF	
A1202/A1203	...	0.29	470.3	r	64.3	FF	
7111/7116	192/193	0.23	283.2	r	18.4	TT	Pairs
7199/7232	196/197	0.56	127.3	r	66.0	TT	
7199/7322	196	1.95	458.5	n	89.8	TF	
7232/7322	197	1.39	371.9	n	23.9	TF	
7249/7260	...	0.26	155.7	r	74.8	FF	
7323/7408	205	0.71	387.6	n	51.4	FT	
7399/7408	205	0.49	276.9	r	73.2	FT	
7513/7557	216	0.37	331.4	r	67.4	FT	
7559/7599	214/218	0.29	81.9	r	60.1	TT	
7559/7605	214/219	1.45	422.8	n	89.0	TT	
7599/7605	218/219	1.50	480.3	n	28.9	TT	
7713/7788	...	1.21	307.6	r	83.6	FF	
7853/7861	235/236	0.14	88.6	r	65.4:	TT	Pairs
7865/7907	239	0.54	350.2	r	32.6	FT	
7884/7902	...	0.29	274.1	r	60.6	FF	
7950/7971	243/246	0.53	307.4	r	35.3	TT	
N4781/N4790	...	0.32	374.1	n	89.7	FF	
N4781/A1252	254	0.32	369.6	n	58.7	FT	
N4790/A1252	254	0.20	236.6	r	31.2	FT	
8053/8054	255	0.30	196.7	r	55.8	TF	
A1259/A1300	258/259	0.34	202.4	r	9.9	TT	
8215/8308	262/272	1.06	287.8	n	54.2	TT	
8215/8249	262/273	1.44	411.7	n	27.3	TT	
8215/8331	262/274	1.42	454.5	n	43.2	TT	
8261/8280	265/267	0.27	236.9	r	39.1	TT	
8303/8307	270/271	0.39	370.5	r	67.7	TT	
8308/8320	272/273	0.43	112.3	r	26.9	TT	
8308/8331	272/274	1.23	358.4	n	97.4	TT	
8320/8331	273/274	1.59	488.0	n	70.5	TT	
8837/8981	295/302	1.33	402.6	n	102.0	TT	
8981/9013	302/304	0.74	275.8	r	35.1	TT	
9753/9776	553/327	0.45	425.7	r	65.7	TT	

[a] Reciprocal or nonreciprocal.

[b] T = Tifft-Cocke; F = Fisher-Tully.

al. 1986), but in the light of this work with third components the ΔV patterns in groups and pairs can be expected to show some differences.

The importance of distinguishing the wider Schweizer pairs ($VS > 300$ km s^{-1} deg) in the quantization testing in § III can now be clarified. Examination of Table 5 shows that in passing from $VS < 300$ km s^{-1} deg to $VS > 300$ km s^{-1} deg, the number of "In" objects shows no significant change (12 : 14) but the number of "Out" objects rises distinctly (5 : 12.5). This corresponds to a dramatic change in the reciprocal/nonreciprocal ratio from 16 : 13 to 1 : 14. The potential for selecting nonphysical pairs or "third" components increases sharply outside of $VS = 300$ km s^{-1} deg. Exactly how to interpret this change, whether to consider it simply contamination of isolated pairs or some aspect of quantum effects, remains under investigation. There is, however, a clear basis for defining a critical test region for close pairs bounded at $VS = 300$ km s^{-1} deg.

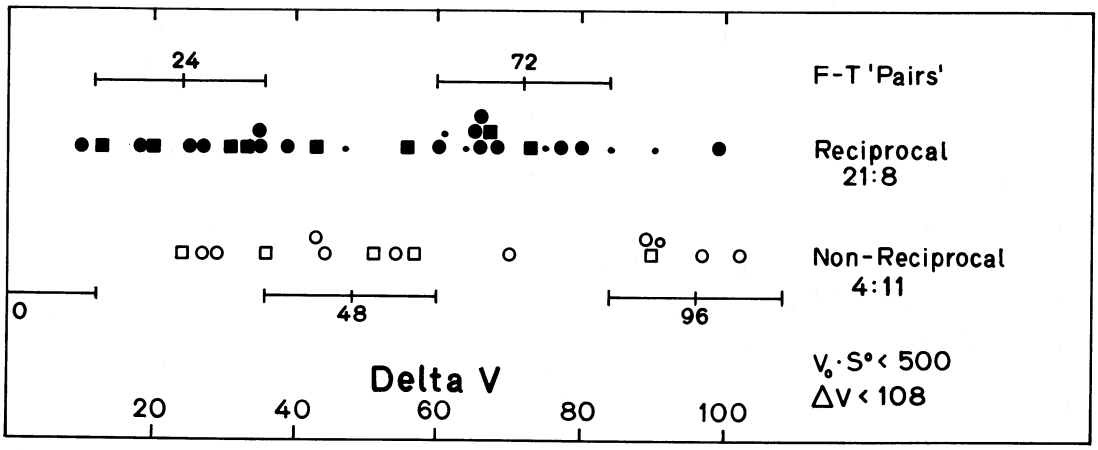

FIG. 6.—ΔV distribution for the 44 pairs in the Fisher-Tully catalog with VS products less than 500 km s^{-1} deg and $\Delta V < 108$ km s^{-1}. Pairs are separated by reciprocity to distinguish primary pair candidates (*filled symbols*) from third-component systems (*open symbols*). Large circles represent differentials formed from new redshifts, while small circles show differentials formed from Fisher-Tully data. Squares combine one redshift from each source.

APPENDIX

COMPARISON OF STEWARD AND KARACHENTSEV REDSHIFT DIFFERENTIALS

The Steward redshift differentials for double galaxies (Tifft 1982*b*) have internally derived uncertainties which are quite small. No precisely equivalent data set exists with which to make an external error evaluation. The most nearly equivalent data set is by Karachentsev (1980). In most cases the Steward data were obtained with an oriented slit to provide a single spectrogram covering both objects. Any exceptions to this procedure are noted. Karachentsev states in his paper that most objects with separations less than 90″ were observed with an oriented slit. Since no specific data are given, it is not possible to verify that this was done for all cases of concern herein. Beyond the common observing technique, the procedures used to derive differential redshifts differ. Karachentsev provides mean redshifts, with internal consistency errors, for each galaxy. If emission is present it is indicated, but no specific information is provided as to what lines entered into a given determination. Final differentials are found by differencing the two redshifts. The only estimate of uncertainty for a particular differential is the combination of the individual internal errors. This provides a minimum error but ignores several effects which will increase the uncertainty. Absolute redshift uncertainties are found by Karachentsev to be about 40 km s^{-1}. Sulentic (1982) finds an absolute uncertainty of 50 km s^{-1} for emission-line redshifts and in excess of 100 km s^{-1} for absorption-line determinations. No analysis of the uncertainties in differentials formed within a common spectrum is available.

Steward differentials were formed when possible by differencing redshift measurements of individual spectral lines in common in both objects, and averaging these differences. Such differentials are called "common-line" (CL) differentials. Individual redshifts within pairs typically contain velocities from lines which are not in common in both objects. Differentials formed from such redshifts are denoted NCL for "non–common-line" differentials. Uncertainty in CL values depends only upon the internal measurements errors for lines, and the uncertainty in referencing the two spectra to a common position with respect to the comparison spectra. This latter uncertainty, called the "tilt" uncertainty, is a simple function of the spacing of the galaxies. Both the measurement and the tilt uncertainties can be estimated internally, and virtually all other sources of error cancel when differences are formed. In generating the Steward CL differentials, line quality was noted, and only differences formed from clear distinct lines were used. Two or more such common lines were required to qualify a system as a "high-weight pair" (HWP). The HWP objects subdivide into CLE, CLA, and CLAE classes according to whether emission, absorption, or a combination was used to form the final mean. Uncertainty will depend upon the type of line used. NCL differentials, including the Karachentsev data, contain the same measurement and tilt uncertainties as well as errors generated by wavelength reference errors from lines not in common, and an admixture of lines of variable quality. NCL uncertainty can therefore be expected to be larger than CL uncertainty.

The ability to detect a periodicity in redshift data is directly related to the uncertainty in the data (Tifft 1982*c*). The Steward differentials were shown to be consistent with predicted (Tifft 1977*a*) redshift quantization at a level consistent with the estimated uncertainties (Tifft 1982*c*). Independent analysis by Sharp (1984) confirmed the presence of the periodicity. Among the high-weight pairs the CLA and CLE classes yield the strongest effect, implying the smallest errors consistent with expectation. CLAE objects were consistent with larger errors. This is expected, since neither emission nor absorption is usually clear and distinct in mixed spectra.

Table 6 contains data on CLE and CLAE pairs which were observed by both Tifft (1982*b*) and Karachentsev (1980). The Karachentsev (1972) identification is followed by the separation in arcseconds. The next two pairs of entries are the Steward and Karachentsev differentials with associated mean errors. The Steward uncertainty is found from equation (3) and Table 6 in Tifft (1982*b*). The Karachentsev value is the combined effect of the two individual uncertainties. The next two columns give the difference between the two differentials and the combined uncertainty. The final column is generated by dividing the differential difference by its uncertainty. The distribution of this last quality provides a means of evaluating the error estimates. If all the given uncertainties were correct, this "error index" would be normally distributed with unit dispersion (Tonry and Davis 1979; Tifft 1982*a*). Rejecting

TABLE 6

DIFFERENTIAL REDSHIFT COMPARISONS

Karachentsev	S	ΔV_T (m.e.) (km s^{-1})	ΔV_K (m.e.) (km s^{-1})	ΔV_{TK} (m.e.) (km s^{-1})	ΔV_{TK}/m.e.
		CLE Comparisons			
1	29″	152 (20)	224 (25)	72 (32)	2.25
5	15	139 (18)	221 (49)	82 (52)	1.58
33	65	14 (27)	227 (23)	213 (35)	6.1[a]
36	23	35 (19)	125 (28)	90 (34)	2.65
39	17	6 (18)	42 (42)	36 (46)	0.78
124	23	145 (19)	88 (71)	57 (73)	0.78
135	12	65 (18)	123 (26)	58 (32)	1.81
137	28	14 (20)	9 (14)	5 (24)	0.21
144	53	15 (24)	103 (34)	88 (42)	2.10
159	80	149 (31)	172 (25)	23 (40)	0.58
161	42	18 (22)	27 (28)	9 (36)	0.25
177	48	79 (23)	19 (23)	60 (33)	1.82
186	52	9 (24)	74 (18)	65 (30)	2.17
206	60	196 (26)	98 (34)	98 (43)	2.28
208	79	3 (31)	28 (18)	25 (36)	0.69
222	64	87 (27)	146 (20)	59 (34)	1.74
227	79	42 (31)	149 (71)	107 (77)	1.39
258	52	41 (24)	38 (21)	3 (32)	0.09
261	65	67 (27)	40 (38)	27 (47)	0.57
292	52	34 (24)	11 (24)	23 (34)	0.68
326	36	124 (21)	56 (14)	68 (25)	2.72
340	12	144 (18)	71 (28)	73 (33)	2.21
362	48	27 (23)	75 (24)	48 (33)	1.45
368	37	59 (21)	50 (28)	9 (35)	0.26
369	36	73 (21)	140 (23)	67 (31)	2.16
370	9	63 (18)	41 (24)	22 (30)	0.73
414	65	17 (27)	40 (48)	23 (55)	0.42
424	22	9 (19)	6 (16)	3 (25)	0.12
446	38	438 (21)	328 (24)	110 (32)	3.44
479	28	89 (20)	22 (33)	67 (39)	1.72
488	19	5 (18)	8 (34)	3 (38)	0.08
518	65	102 (27)	103 (25)	1 (37)	0.03
536	25	237 (19)	219 (46)	18 (50)	0.36
540	62	140 (26)	87 (14)	53 (30)	1.77
551	58	20 (25)	8 (39)	12 (46)	0.26
560	6	260 (18)	127 (22)	133 (28)	4.8[a]
603	70	25 (28)	57 (19)	32 (34)	0.94
		CLAE Comparisons			
13	24	57 (19)	178 (42)	121 (46)	2.63
73	25	198 (19)	104 (63)	94 (66)	1.42
129	75	132 (30)	176 (60)	44 (67)	0.66
146	12	156 (18)	239 (55)	83 (58)	1.43
160	85	719 (33)	774 (28)	56 (43)	1.30
204	15	20 (18)	50 (16)	30 (24)	1.25
248	48	333 (23)	274 (31)	59 (39)	1.51
293	56	182 (25)	213 (21)	31 (33)	0.94
335	20	179 (19)	132 (71)	47 (73)	0.64
383	26	7 (19)	43 (39)	18 (43)	0.42
401	27	136 (19)	46 (38)	90 (42)	2.14
406	72	118 (29)	93 (21)	25 (36)	0.69
423	75	223 (29)	68 (20)	155 (35)	4.43
439	53	2 (24)	146 (45)	144 (51)	2.82
490	47	45 (23)	144 (24)	99 (33)	3.00
524	53	186 (24)	196 (28)	10 (37)	0.27

[a] Reject.

two CLE points, which fall well outside expectations for their associated distributions, the distributions are well characterized as normal distributions. The dispersion is, however, larger than unity. The total CLE and CLAE samples have dispersions of 1.5 and 1.9, respectively. The estimated errors cannot be correct in all cases.

As noted earlier, the Steward errors refer to the actual differential, but the Karachentsev errors do not. We may easily illustrate this by sorting the pairs according to the size of the Karachentsev error estimate. If the estimates actually reflected the quality of the differentials, which in fact is largely determined by the strength and clarity of the emission lines, the same trend should be present in the Steward data. The scatter in comparing Karachentsev and Steward values should increase in proportion, and the distribution of the error index should be unchanged. Table 7 gives ordered error index distributions for all CLAE objects and CLE objects with

TABLE 7

DISTRIBUTION OF $\Delta V_{TK}/(\text{m.e.})_{TK}$ FOR CLE AND CLAE PAIRS AT VARIOUS $(\text{m.e.})_K$ LEVELS

CLE		
$(\text{m.e.})_K > 25$	$(\text{m.e.})_K < 25$	CLAE
0.03	0.09	0.27
0.08	0.12	0.42
0.25	0.21	0.64
0.26	0.68	0.66
0.26	0.69	0.69
0.36	0.73	0.94
0.42	0.94	1.25
0.57	1.45	1.30
0.58	1.74	1.42
0.78	1.77	1.43
0.78	1.82	1.51
1.39	2.16	2.14
1.58	2.17	2.63
1.72	2.25	2.82
1.81	2.72	3.00
2.10	3.44	4.43
2.21	...	...
2.28	...	...
2.65	...	...
1.35[a]	1.72[a]	1.94[a]

[a] rms dispersion (discrepancy index).

Karachentsev error estimates greater or less than 25 km s^{-1}. The rms dispersion of each distribution is given at the bottom and will subsequently be called the "discrepancy index." The CLE discrepancy index changes in step with the Karachentsev error estimate. The Karachentsev error estimates cannot be related to the actual quality of the differentials to a high degree.

Table 8 summarizes the Steward-Karachentsev comparisons for the full range of uncertainty. Each value is followed by the number of pairs involved, given in parentheses. The center columns give the breakdown of the CLE pairs in angular separation, which relates to the Steward uncertainties. The figures at the bottom give the actual rms deviations between Steward and Karachentsev data in kilometers per second. This deviation is not dependent on separation and actually decreases slightly, but not significantly, as separation increases. Uncertainty in CLAE pairs is obviously greater, as anticipated.

As noted earlier, the uncertainty in a differential cannot be less than the combined errors of the individual redshifts. Table 8 shows that the discrepancy index for CLE pairs goes to unity for Karachentsev error ranges above 35 km s^{-1}. Any significant increase in Steward uncertainty to account for part of the discrepancy at smaller Karachentsev deviations will force the index below unity for the larger deviations. This is not possible if the Karachentsev redshift error figures are real internal scatter. No significant increase in Steward uncertainty for CLE objects appears possible. One possible clue as to why the discrepancy varies as it does may be found in the separation distribution data in Table 8. There is a trend toward wider spacings as the discrepancy increases. The size of the deviation will therefore decrease if tilt uncertainty is added to the Karachentsev error estimates. An even larger effect would be produced if the basic tilt corrections themselves, to refer the spectrum of each galaxy to the same slit position as the mean comparison spectrum, were not applied properly.

In summary, we find the Steward-Karachentsev comparison to be consistent with the Steward errors as stated for CLE pairs.

TABLE 8

SUMMARY OF STEWARD-KARACHENTSEV ERROR DISCREPANCY AS A FUNCTION OF KARACHENTSEV ERROR LEVEL

Level	Discrepancy (N)[a] (CLE)	Number of Pairs with S $<40'':>40''$	Discrepancy (N)[a] (CLAE)
$(\text{m.e.})_K > 45$	1.03 (5)	...	...
$(\text{m.e.})_K > 35$	0.89 (8)	...	1.75 (8)
$(\text{m.e.})_K$ *all*	...	...	1.94 (16)
$(\text{m.e.})_K < 35$	...	...	2.11 (8)
$(\text{m.e.})_K > 25$	1.35 (19)	11:8	...
$(\text{m.e.})_K$ *all*	1.52 (35)	17:18	...
$(\text{m.e.})_K < 25$	1.72 (16)	6:10	...
$(\text{m.e.})_{KT}$ (km s^{-1})	56 (35)	...	82 (16)

[a] N = number of pairs involved.

Karachentsev errors are typically near 45 km s^{-1} for the same pairs. It is incorrect to judge the differential quality by the internal scatter in the individual redshifts without allowing for additional effects. Errors in CLAE pair differentials are clearly larger than for CLE pairs.

REFERENCES

Arp, H. 1986, *Astr. Ap.*, **156**, 207.
Arp, H., and Sulentic, J. W. 1985, *Ap. J.*, **291**, 88.
Cocke, W. J., and Tifft, W. G. 1983, *Ap. J.*, **268**, 56.
Fisher, J. R., and Tully, R. B. 1981, *Ap. J. Suppl.*, **47**, 139.
Karachentsev, I. D. 1972, *Comm. Sp. Ap. Obs. USSR*, **7**, 1.
———. 1980, *Ap. J. Suppl.*, **44**, 137.
Napier, W. M. 1988, in *Proc. Symposium on New Ideas in Astronomy* (Venice) (Cambridge: Cambridge University Press).
Peterson, S. D. 1979, *Ap. J. Suppl.*, **40**, 527.
Picchio, G., and Tanzella-Nitti, G. 1985, *Astr. Ap.*, **142**, 21.
Sadler, E. M., and Sharp, N. A. 1984, *Astr. Ap.*, **133**, 216.
Schneider, S. E., Helou, G., Salpeter, E. E., and Terzian, Y. 1986, *A.J.*, **92**, 742.
Schweizer, L. Y. 1987, *Ap. J. Suppl.*, **64**, 427.
Sharp, N. A. 1984, *Ap. J.*, **286**, 437.
Sulentic, J. W. 1982, *Ap. J.*, **252**, 439.
Tifft, W. G. 1976, *Ap. J.*, **206**, 38.
———. 1977*a*, *Ap. J.*, **211**, 31.
———. 1977*b*, *Ap. J.*, **211**, 377.
———. 1980, *Ap. J.*, **236**, 70.
———. 1982*a*, *Ap. J.*, **257**, 442.
———. 1982*b*, *Ap. J. Suppl.*, **50**, 319.
———. 1982*c*, *Ap. J.*, **262**, 44.
———. 1988, in *Proc. Symposium on New Ideas in Astronomy* (Venice) (Cambridge: Cambridge University Press).
Tifft, W. G., and Cocke, W. J. 1984, *Ap. J.*, **287**, 492.
———. 1988, *Ap. J. Suppl.*, **67**, 1.
Tonry, J., and Davis, M. 1979, *A.J.*, **84**, 1511.
Turner, E. 1976, *Ap. J.*, **208**, 20.
White, S., Huchra, J., Latham, D., and Davis, M. 1983, *M.N.R.A.S.*, **303**, 701.

W. J. Cocke and W. G. Tifft: Steward Observatory, University of Arizona, Tucson, AZ 85721